Available online at www.sciencedirect.com
ScienceDirect
Earth and Planetary Science Letters 249 (2006) 62–73
EPSL
www.elsevier.com/locate/epsl

Support of high elevation in the southern Basin and Range based on the composition and architecture of the crust in the Basin and Range and Colorado Plateau

Andy Frassetto [a,*], Hersh Gilbert [a], George Zandt [a], Susan Beck [a], Matthew J. Fouch [b]

[a] Department of Geosciences, University of Arizona, Gould-Simpson Building #77, 1040 E 4th St., Tucson, AZ 85721, USA
[b] Department of Geological Sciences, Arizona State University, Box 871404, Temple, AZ 85287-1404, USA

Received 17 February 2006; received in revised form 26 June 2006; accepted 27 June 2006

Editor: R. D. van der Hilst

Abstract

To explore the nature of how the structure and physical properties of the crust vary from extended to relatively unextended domains we present teleseismic receiver functions which measure crustal thickness, shear wavespeed structure and the Vp/Vs ratio at 12 seismic stations in eastern Arizona. The crustal thickness is ~28 km, increases slightly eastward, and remains nearly uniform beneath the varying elevations in the southern Basin and Range. The observed Vp/Vs ratio in the Basin and Range (~1.78) exceeds the global average. The southern Colorado Plateau exhibits thicker crust (~40 km) and a slightly greater observed Vp/Vs (~1.81). A discrete region in the Colorado Plateau generates an unusually high Vp/Vs ratio (1.90) and contains low wavespeed zones which serve as evidence of partial melt related to Quaternary volcanism. The metamorphic core complexes in the southern Basin and Range likewise exhibit anomalously high Vp/Vs values (1.79–1.87) and lack locally compensating crustal roots. Density models show that ~85 kg/m^3 lighter crust or ~35 kg/m^3 lighter mantle than that of the surrounding Basin and Range helps these metamorphic core complexes maintain their high elevation. Compositional modeling of intrusive bodies exposed throughout the Catalina–Rincon metamorphic core complex indicates that the observed high Vp/Vs ratio and modeled low density could result from substantial amounts of a plagioclase-rich, quartz-poor rock. These Vp/Vs data are evidence that significant compositional heterogeneity of the crust can occur over a short distance and provide a clue as to how these areas that underwent significant Tertiary extension may have been preconditioned for orogenic collapse.

Keywords: Vp/Vs ratio; receiver function; metamorphic core complex; isostasy; Basin and Range; Colorado Plateau

1. Tectonic setting and broadband deployment

Southwestern North America has been tectonically modified to an extreme degree since the Mesozoic; from the late Cretaceous to early Tertiary (~80–40 Ma) the shallowing dip of the subducting Farallon slab shifted magmatism inboard of the arc and promoted Laramide crustal thickening throughout the Cordillera (see Dickinson [1] for a summary). The subsequent orogenic collapse in the middle Tertiary extended and exhumed mid-crustal metamorphic and igneous rocks from within the overthickened crust forming metamorphic core complexes (MCCs) in the Basin and Range [2]. Continued extension and magmatism persisted during the transition to a transform boundary as the Farallon

* Corresponding author. Tel.: +1 520 730 6731; fax: +1 520 621 2672.
E-mail address: andyf@geo.arizona.edu (A. Frassetto).

0012-821X/$ - see front matter © 2006 Elsevier B.V. All rights reserved.
doi:10.1016/j.epsl.2006.06.040

plate was subducted (see Sonder and Jones [3] for a review). Meanwhile unresolved factors allowed uplift of the Colorado Plateau to its present elevation without imparting significant internal deformation. The Cenozoic collapse of the Cordillera and its linkage to the current structure, composition, and form of support for the high elevations of both the Colorado Plateau and the Basin and Range remains a controversial issue that is fundamental to understanding the tectonic development of western North America.

Here we present a teleseismic receiver function analysis using data from a recent regional broadband seismic deployment. These observations effectively constrain the Poisson's ratio (or Vp/Vs) of the crust, allow us to identify layers of differing shear wavespeed and measure crustal thickness, and provide a vital framework to interpret the evolution of the Cenozoic extensional domain in western North America. In particular we hope to further constrain the forces which drive the profound changes in elevation and topography that are observed from the Basin and Range to the Colorado Plateau (e.g., [4]). To this end we use the receiver function method to characterize the crust and upper mantle in the region, produce constraints necessary to broadly explore the composition of the crust, and model the density distribution in the upper lithosphere to examine the sources that compensate high elevation in the southern Basin and Range.

The **Co**nsortium for an **A**rizona **R**econnaissance **S**eismic **E**xperiment (**COARSE**) deployment of nine broadband seismometers spans the three main tectonic provinces of Arizona in an approximate SW–NE swath (Fig. 1). Arizona State University's ASU seismograph, National Seismic Network station WUAZ, and Global Seismic Network station TUC are included to improve array coverage.

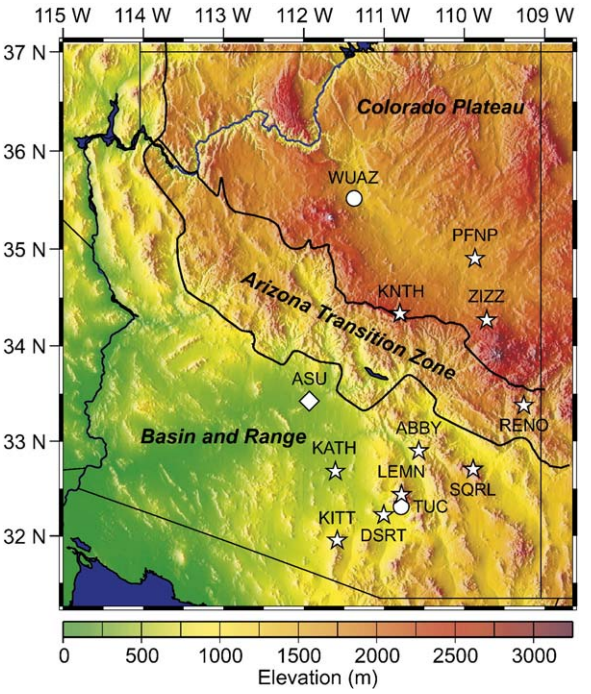

Fig. 1. The COARSE deployment (2003-Present) across eastern Arizona. All sites (excluding KATH) are near bedrock and produce high quality broadband earthquake recordings. For additional information visit http://asuarray.asu.edu/coarse/index.php.

2. Teleseismic receiver function analyses

To analyze the structure of the crust and uppermost mantle beneath COARSE array stations we compute high quality teleseismic receiver functions with the iterative pulse stripping time domain deconvolution technique (Fig. 2) [5]. During this process the vertical P wave energy is deconvolved from the horizontal (radial and tangential) components, removing source effects and preserving only near receiver P–SV and P–SH converted phases which are generated by structure in the lithosphere beneath each seismic station [6,7]. This study focuses on the P–SV (hereafter called Ps) converted phases of the radial component which are most sensitive to large scale variability in the shear wavespeed structure. Frequency content of our receiver functions from 0.05 Hz to 2.5 Hz allows for resolution of Ps phases from layer thicknesses of greater than ~0.5 km. The amplitude of a Ps phase depends on the wavespeed contrast at a layer boundary. Negative Ps polarities characterize higher to lower wavespeeds with increasing depth, while positive polarities characterize lower to higher wavespeeds (Fig. 2). We refer to the amplitude of a Ps as a percentage of its amplitude to that of normalized initial P pulse. To analyze the highest quality results we accept receiver functions only if they satisfy a variance reduction cutoff above 80% and retain their highest amplitude, the direct P, within one second of the zero time on the deconvolved trace. Direct P sources are selected from epicentral distances of 30 to 90° and yield a dataset where most events are clustered in northern and southwestern Pacific subduction zones, as well as in Central and South America.

Analyses of these data in the depth domain allow for the most accurate tectonic interpretation. To accomplish this and to produce a robust seismic characterization we eliminate one major unknown by assuming a standard Vp for the entire crust. We use a wavespeed of 6.2 km/s developed by Christensen and Mooney [8] in their review of crustal seismic observations from extensional

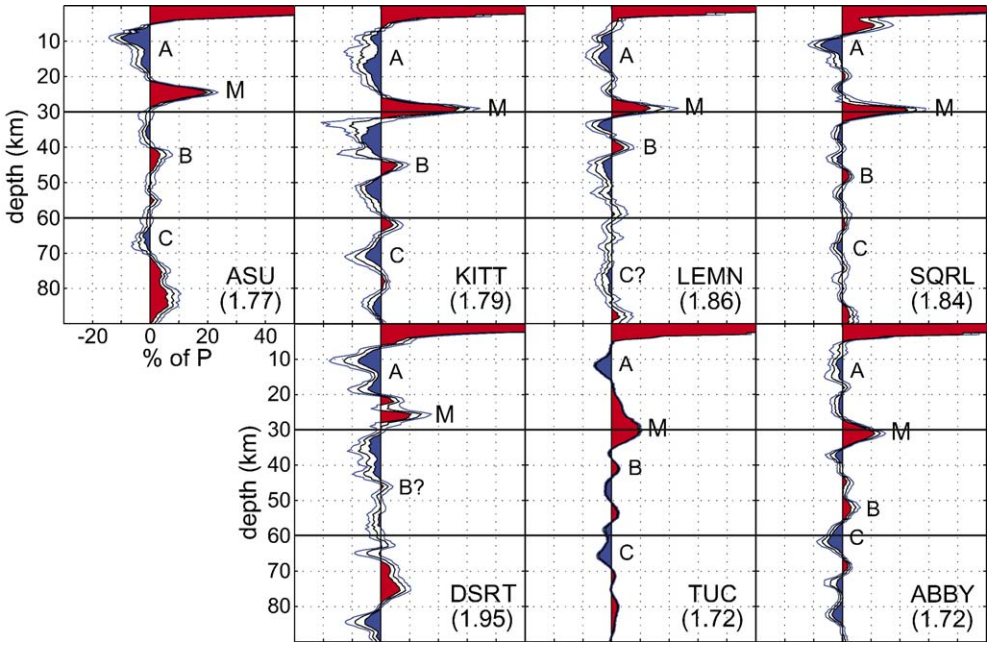

Fig. 2. Stacked Basin and Range receiver functions, grouped by Moho amplitude and Vp/Vs. Commonly observed interfaces have been identified with labels. M represents the estimated Moho.

domains. Numerous refraction experiments throughout the Basin and Range—Colorado Plateau transition zone also measure a bulk crustal Vp of 6.2±0.1 km/s [9–12]. This value also matches observations for the southern Colorado Plateau [13]. A range of wavespeeds between 6.1–6.3 km/s is probable based on the variety of geologic environments sampled by COARSE and the uncertainty in the refraction results. Tests on COARSE data show that variations in Vp have negligible effects on the observed Vp/Vs ratio and alter crustal thickness estimates by only ±0.5 km for Vp changes of ±0.1 km/s. Thus minor deviations from our constant Vp model do not significantly affect the overall findings.

We evaluate the primary Ps phase and its multiples by using the thickness—Vp/Vs domain phase stacking algorithm (Fig. 3) [14]. This stacking technique allows us to map the convergence of the direct Ps and its PpPs and PpSs+PsPs multiples for the Moho interface in order to estimate the crustal Vp/Vs and thickness beneath our stations. With ideal convergence a point of maximum

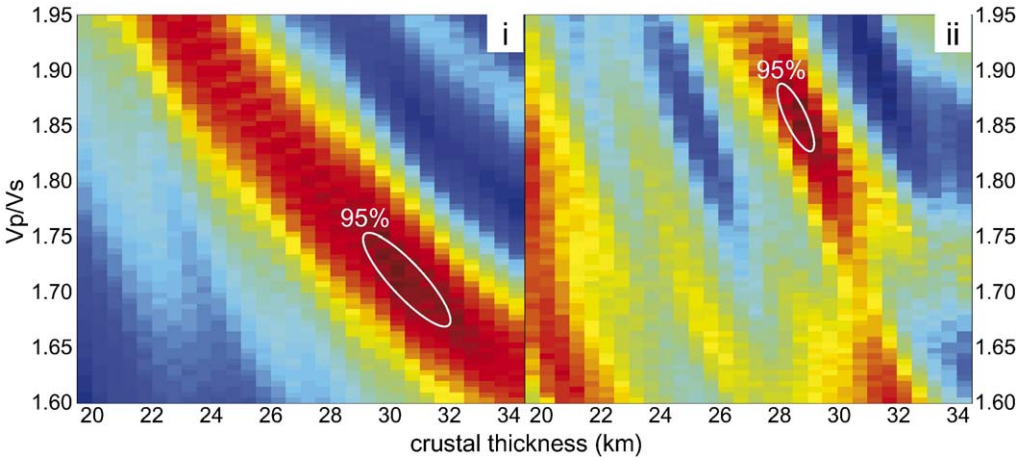

Fig. 3. Vp/Vs-thickness relation from phase stacks of: (i) receiver function azimuths (90–300°) sampling beneath the Tucson Basin and (ii) azimuths (300–90°) sampling beneath the Catalina–Rincon MCC.

Table 1
Elevation, crustal thickness and Vp/Vs (with uncertainty range at 95% of maximum stacked amplitude) for Basin and Range stations

Station	Elevation (m)	Thickness (km)	Vp/Vs	Events
ABBY	794	31 (31–33)	(1.74–1.68) 1.72	64
ASU	364	24.5 (24–25.5)	(1.80–1.74) 1.77	34
DSRT[a, b]	802	25.5 (25–27.5)	(1.95–1.90) 1.95	28
KITT	1467	27.5 (25.5–28.5)	(1.86–1.76) 1.79	49
LEMN	2489	29 (28.5–30)	(1.89–1.84) 1.86	21
SQRL	3085	29 (28–29.5)	(1.87–1.84) 1.84	36
TUC[c]	874	30 (29–32)	(1.75–1.67) 1.72	270
TUC[d]	874	28.5 (28–29)	(1.89–1.82) 1.87	117

Tradeoff between crustal thickness and Vp/Vs ratio exhibits that the lowest allowable thickness corresponds to the greatest Vp/Vs within the maximum amplitude bounds. Uncertainty range does not account for variations in Vp.
[a] Azimuthal heterogeneity and/or significant noise present.
[b] 90% maximum amplitude contour used.
[c] Azimuths (90–300°) sampling beneath the Tucson Basin.
[d] Azimuths (300–90°) sampling beneath the Catalina–Rincon MCC.

amplitude or "bull's-eye" signifies the most likely solution. The inherent weakness in this technique, the tradeoff between crustal thickness and Vp/Vs which leads to a diagonal smearing of the bull's-eye, produces some uncertainty in both the crustal thickness and Vp/Vs solutions. Additionally the peak amplitude of the stacked phases is often asymmetrically located within a larger zone of high amplitude. In order to constrain the confidence in our picks we determine the width of the maximum amplitude range and accept any solution within 95% (or 90% at stations DSRT, KNTH, ZIZZ) of the peak amplitude. This produces a range of estimates encompassing the maximum convergence that represent the uncertainty in our results (Tables 1 and 2).

To verify these measurements we plot the moveout of phase arrivals as a function of ray parameter [15]. Moveout accounts for the differential arrival time of direct or converted waves plotted as a function of ray parameter. Direct Ps arrivals exhibit positive moveout with respect to the direct P arrival with increasing ray parameter while the ray geometry of PpPs and PpSs +PsPs multiples produces a negative moveout. Thus we can predict and compare expected and observed moveout on receiver functions in order to verify that the arrival of Ps phases and their later multiple reverberations are produced at particular depths. The identification of later phases is critical prior to interpretation of seismic structure because it allows us to discriminate between direct arrivals and multiples that may be spuriously interpreted. Receiver functions from each station are corrected for moveout, stacked to improve the observed signal, and migrated to depth using the measured Vp/Vs to determine the depth of the Moho.

3. Receiver function observations and interpretations

Although the event count at some stations is small, at least 21 receiver functions pierce the crust and upper mantle within several kilometers of each location. Azimuthal distribution of seismicity reveals a considerable gap in sampling towards the N and E where few suitable teleseismic earthquakes are generated. Despite these hindrances we record pronounced and systematic trends in the receiver functions sampling within each tectonic region. Within solely the Basin and Range we view interesting variations between stations located on MCC summits and those located in less extended regions.

3.1. Basin and range

Receiver functions for the Basin and Range (Fig. 2) contain similar features for most stations. At 6–20 km depth we find a broad negative Ps (labeled A in figure) of 5–10% that is indicative of the top of slow wavespeed material, perhaps due to the presence of high temperatures, partial melt or a shear zone. The negative arrival is most pronounced near the MCCs and is entirely absent at ABBY, the only station to sample a relatively undeformed region, suggesting that it may result from extension. A well-defined Moho Ps (M) arrives from depths of 24.5–31 km. With the exception of the especially thin crust at ASU crustal thickness remains similar throughout the region and is comparable to thicknesses estimated from previous refraction profiling [10,11].

Moho amplitude varies significantly. Stations located at low elevation (ABBY, DSRT, TUC) record a uniformly

Table 2
Elevation, crustal thickness and Vp/Vs (with uncertainty range at 95% of maximum stacked amplitude) for Colorado Plateau stations

Station	Elevation (m)	Thickness (km)	Vp/Vs	Events
KNTH[b]	2286	41.5 (41–42)	(1.78–1.73) 1.76	71
PFNP	1759	39.5 (38.5–41)	(1.79–1.73) 1.76	35
RENO	1909	36.0 (34.5–36.5)	(1.86–1.81) 1.82	36
WUAZ	1592	43.5 (43–44.5)	(1.92–1.88) 1.90	165
ZIZZ[a, b]	2011	43 (42–43)	(1.71–1.67) 1.68	44

Tradeoff between crustal thickness and Vp/Vs ratio exhibits that the lowest allowable thickness corresponds to the greatest Vp/Vs within the maximum amplitude bounds. Uncertainty range does not account for variations in Vp.
[a] Azimuthal heterogeneity and/or significant noise present.
[b] 90% maximum amplitude contour used.

weak Moho amplitude (~10%). This small amount of converted energy may result from a reduced shear wavespeed and/or density contrast across the crust–mantle interface. The Moho Ps beneath or near the South Mountain, Baboquivari, Catalina–Rincon and Pinaleño MCCs (stations ASU, KITT, LEMN, SQRL respectively) is considerably greater (15–30%) suggesting a more rapid transition from crust to mantle or a larger impedance contrast at the base of the crust; either slow or low density crust atop normal mantle or alternatively normal lower crust atop fast or high density mantle.

The receiver functions show few converted phases below the Moho Ps. There is evidence of a diffuse 5% positive Ps (B) at 40–55 km beneath all stations except DSRT (Fig. 2). Noise may obscure this interface at DSRT and the layer is probably characteristic of the region and would represent an abrupt increase in shear wavespeed at ~15–20 km below the Moho. This may signify an increase with depth from the low Pn wavespeeds of 7.67–7.85 km/s observed previously [10–12]. We also notice a 5–7% negative Ps (C) that appears at most stations at 60–75 km and corresponds to a decrease in shear wavespeed in the upper mantle. Moveout analysis verifies that neither this nor the earlier arrival result from the reverberations of shallower layers. Therefore these observed Ps conversions from interfaces marked by B and C bound a ~20–25 km thick layer of relatively dense or fast mantle that underlies the southern Basin and Range. Additional weak Ps observed beneath the Moho result from a combination of reverberations from the shallow negative Ps and assorted small Ps from the upper mantle.

Crustal thickness and Vp/Vs estimates (Table 1) show pronounced variability amongst Basin and Range stations. Stations KITT, LEMN and SQRL show no increase in crustal thickness, an unexpected result for being situated atop high and large ranges, and contain anomalously high Vp/Vs values. The lack of a crustal root beneath LEMN differs from the interpretations by Myers and Beck [16], who detect an apparent deepening of the Moho at nearby TUC from receiver functions that sample beneath the higher elevations. Now with sufficient data to explore the Vp/Vs-thickness relation, we offer an alternative explanation that the apparent crustal thickening beneath the Catalina–Rincon MCC may result from a significant azimuthal variation of the crustal Vp/Vs ratio on a local scale. We evaluate this shift with the phase stacking technique by using 270 receiver functions that sample outside the MCC and 171 that sample in a narrow swath beneath the range (Fig. 3). This distribution and density of receiver functions reveals a strong zonation in the Vp/Vs with a low value (1.71) measured external of the MCC compared to a much higher Vp/Vs ratio (1.87) detected beneath it (Table 1). This result is also consistent with the high value (1.86) observed at site LEMN located at the summit of the MCC. In fact the average Vp/Vs measurement of all MCCs is greater (1.83) than remaining Basin and Range stations (1.73) ignoring station DSRT. Measurements at ABBY and TUC curiously exhibit equal or slightly thicker crust than the higher elevation MCCs sampled at KITT, LEMN and SQRL. The thinnest crust surveyed at ASU also exhibits a higher Vp/Vs (1.77), which may arise from its proximity to the South Mountain MCC, but we currently lack sufficient data to evaluate its Vp/Vs characteristic azimuthally in the same manner as achieved at TUC. Important to note is DSRT which is sited at a noisy location in the Tucson Mountains. The data show an outlier Vp/Vs of 1.95 for this station, which recorded for only a short duration in a high noise environment. For this reason we exclude this station from any overarching analysis and interpretation of Vp/Vs trends.

Zandt and Ammon [17] measured the global crustal average for Vp/Vs in Mesozoic–Cenozoic orogenic belts to be 1.73, below our average (1.78). However non-MCC Vp/Vs estimates of 1.73 imply that overall Basin and Range crust matches the global average while the MCC value (1.83) may result from the presence of partial melt or a significant shift in crustal composition. The partial melt scenario is unlikely because of the current tectonic quiescence of MCC systems and lack of Neogene volcanism in the area [18]. The presence of mafic material would support a model for sizeable mantle input during MCC formation [19]. However analysis by Christensen [20], which illustrates the dependence of Poisson's ratio on mineral assemblage, describes the significant influence that plagioclase content has on the Vp/Vs ratio of a rock. While the sodium plagioclase end-member (albite) has a relatively lower Vp/Vs (~1.81), the calcium end-member (anorthite) has a very high Vp/Vs (~1.92). Thus the increasing presence of calcic-rich plagioclase will drive the Vp/Vs ratio of a crustal rock above the average value for orogenic belts and may be responsible for the elevated values observed here.

These findings bring into consideration an alternative interpretation for post-Laramide tectonics; that the style of collapse of the Cordillera may have been controlled by spatial variations in the composition of the crust, as evidenced today by this divide of Vp/Vs estimates between these different geologic environments. Also important and possibly connected is the absence of compensating roots beneath MCCs in the southern Basin and Range. This finding suggests that the traditional linear relation between elevation and crustal thickness is invalid here and that these edifices are supported via other means.

3.2. Colorado plateau and Arizona transition zone

Receiver functions in the Colorado Plateau and Transition Zone are characterized by substantially greater seismic heterogeneity than the Basin and Range. We observe numerous Ps phases other than the Moho that possess high amplitude throughout the crust and upper mantle (Fig. 4). In addition all receiver functions appear to contain a direct P that is offset from 0 km. This is probably the result of the estimated 2–3 km of seismically slow sedimentary rocks that cap most of the Colorado Plateau and are exposed in the Grand Canyon. The base of this layer creates a large near surface Ps that interferes with and slightly shifts the direct P arrival.

Crustal thickness ranges from 36–43.5 km throughout the region (Table 2). Observed Ps from the Moho (M) are similar throughout the region (~10% of the direct P) and generally smaller than in the Basin and Range with an exception at RENO (20%) (Fig. 4). Additional direct Ps phases disclose substantial stratification and seismic heterogeneity in the crust. Stations KNTH, WUAZ and ZIZZ contain a large (10–15%) mid-crustal arrival (B) from 15–25 km that is the bottom of a slow wavespeed layer. At deeper levels in the crust WUAZ contains a Ps (C) above the Moho at 34 km. Stations KNTH and ZIZZ both exhibit a sub-Moho Ps (D) at 48–54 km which illustrates a further increase in wavespeeds. The COCORP and PACE controlled source seismic profiling experiments identify an interface in this depth range and interpret it as possible deep Moho beneath sections of the Colorado Plateau [13,21]. Locations where we observe the unusual converted phase appear to be limited to volcanic centers and this feature may result from magmatic migration through the lower crust and upper mantle. The complex pattern of several arrivals near, and just below, the Moho at these stations suggests that at localized regions in the Colorado Plateau the crust–mantle transition may be layered or more gradational (Fig. 4). A previous study of upper mantle wavespeed measures a well-constrained Pn of ~8.12 km/s beneath the Plateau. Thus a crust–mantle boundary with multiple layers would minimize a potentially large impedance contrast between crust and relatively fast mantle and produce a similar receiver function response to our observations. Receiver functions at KNTH and WUAZ distinctly express two converted phases with consistent arrival times at all azimuths, casting doubt on the possibility that this intriguing feature results from stacking azimuths which sample the Moho at different depths. Careful examination of the phase stacked plots at KNTH, WUAZ and ZIZZ reveal that despite larger areas of high amplitude generated by the complicated crustal structure, the convergence peak interpreted as M contains amplitudes that are at least 5% greater than

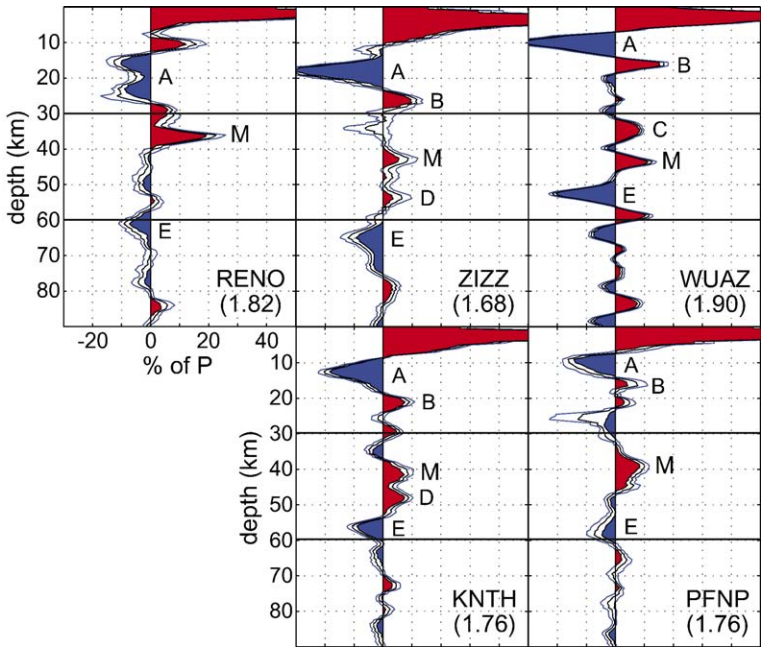

Fig. 4. Stacked Colorado Plateau receiver functions, grouped by structural trends and proximity to volcanic centers. Commonly observed interfaces have been identified with labels. M represents the estimated Moho.

the next highest peak. Furthermore, these peaks provide estimates of crustal thickness close to that found at PFNP which possesses a single peak.

In the uppermost mantle a 7–22% negative Ps (E) appears at 53–65 km beneath the survey area. Its magnitude is strongest beneath KNTH, WUAZ and ZIZZ. This intriguing feature may signal a partial melt zone in the upper mantle which feeds recent volcanism witnessed along the southern margin of the Plateau. Additionally a negative Ps (A) at 10–20 km with 15–30% amplitude (Fig. 4) everywhere except RENO appears to be a PpSs+PsPs reverberation from the sediment cap. At stations WUAZ and ZIZZ however the amplitude is nearly 30% and moveout analysis does not conclusively prove it to be reverberated energy. Its presence as a first-order structure may be explained by a zone of slow wavespeed created by partial melt in the crust. These large negative arrivals are similar to ones associated with the Altiplano–Puna magma body in South America [22] and the Socorro magma body in the Rio Grande Rift [23].

Phase stacking and moveout analyses indicate an average Vp/Vs ratio of 1.81 for Colorado Plateau stations, noticeably higher than the non-MCC related Basin and Range and global average Vp/Vs values and possibly indicative of greater mafic material or partial melt within the crust (Table 2). Separate results from Gilbert et al. [24] also support this observation. WUAZ possesses an unusually high Vp/Vs value (1.90) in addition to the large negative Ps following the Moho which suggests a slow wavespeed region in the upper mantle. When viewed in proximity to the nearby volcanic centers it provides possible evidence for the presence of partially molten crust and upper mantle near the currently active San Francisco Volcanic Field [25]. Azimuthal variability of the Ps phases displays reduced amplitudes within a zone near the most recent volcanism at Sunset Crater. Melt dominated material in the mid- to upper-crust may be responsible for the reduction in converted energy. These findings coincide with the location of substantial volumes of Quaternary volcanism viewed along the Colorado Plateau rim and in the Arizona transition zone [18,26]. Unlike WUAZ, ZIZZ does not have a definitive and station-wide increase in Vp/Vs ratio that indicates melt, but instead shows substantial noise and azimuthal heterogeneity which makes a reasonable Vp/Vs value difficult to constrain. Like DSRT we have excluded the Vp/Vs ratio at ZIZZ from broader interpretations.

Although crustal thickness, isostatic support and means of uplift for the Colorado Plateau are thoroughly debated and the subject of numerous studies (e.g., [27–32]) no model manages to unify the numerous seismic, gravity and heat flow observations for the region. With our deployment we provide new seismic observations (Fig. 4) for the Colorado Plateau which help clarify our understanding of the region. The range of crustal thickness estimates (36–43.5 km) generally matches those from previous geophysical investigations that found crust of ~35–42 km in nearby regions [13,33]. Both the upper mantle low velocity zone [34] and layered crust [35] previously seen across the central and western Colorado Plateau are present in measurements here. The weak Moho Ps and large negative upper mantle Ps indicating relatively slow upper mantle wavespeed beneath the study area concurs with the calculation by Roy et al. [30] for a layer of lower density upper mantle residing beneath the Plateau's eastern edge. All COARSE stations demonstrate thick and stratified crust beneath the Colorado Plateau. The exact cause for this zone of substantial shear wavespeed variation is unknown, but the layering and high average Vp/Vs ratio may be linked to the hypothesis of crustal growth via magmatic addition [29].

4. Support of high elevation in the Basin and Range

The complex and surprising nature of seismic observations for the southern Basin and Range warrants further consideration and is the primary focus here. Estimated depth for the Moho beneath the MCCs clearly deviates from the traditional linear relationship between crustal thickness and elevation (Fig. 5). An Isostatic Residual Gravity Map by Simpson et al. [36] shows variation of the

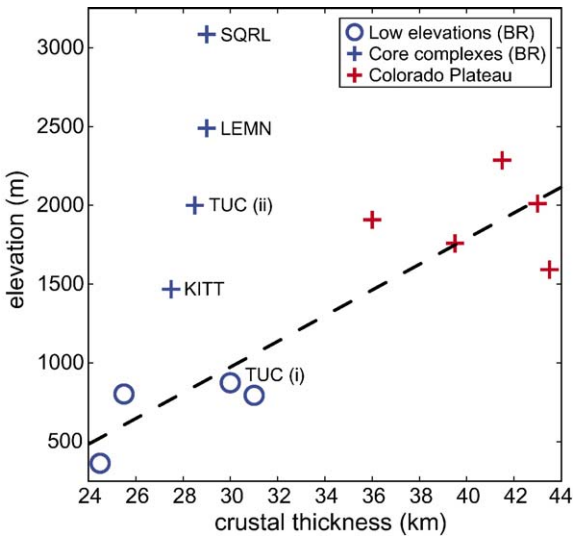

Fig. 5. Relationship of elevation and crustal thickness for COARSE stations. A least squares trend-line is fit to all stations with the exclusion of those atop MCCs. Data from TUC is divided in the same manner as in Fig. 3.

calculated isostatic anomaly due to the presence or absence of an Airy root. An anomaly of zero mgal serves as evidence that the region is balanced by a root necessary to account for the observed elevation and Bouguer gravity anomaly. Negative or positive excursions result from a corresponding mass deficit or surplus created by the correction. Stations ABBY, DSRT and TUC coincide with anomalies of approximately zero mgal while KITT, LEMN and SQRL exist within 20–30 mgal lows. These low values demonstrate that the isostatic correction is too large and when compared with receiver function data support our observation that none of the MCCs surveyed by COARSE are supported by a crustal root.

4.1. Density models

Even geodynamic models that use a flexural response to support MCC elevation still require a local thickening of the crust approaching 10 km to compensate for the observed elevation [37]. We investigate the possibility that lower density crust may allow for high elevation without a corresponding crustal root. To test this hypothesis we use the ISOBAL isostasy modeling program [Clem Chase, personal communication]. This software balances a user specified reference column against a model with density or layer thickness allowed to vary, and also calculates a 1D Bouguer anomaly for each column. For this analysis we test three crustal reference models and use them to calculate the corresponding crustal density of the Catalina–Rincon MCC (Fig. 6). For the MCC, we hold the seismically determined crustal thickness (29 km), the approximate average elevation (1.8 km), and the estimated density of the mantle (3250 kg/m^3) fixed. We then balance the two columns and adjust the crustal density until it matches the observed difference between the Bouguer gravity anomalies each location [38]. This final step is needed to account for the linearly trending, long wavelength decrease in the Bouguer gravity field across southern Arizona [33].

Two of the reference cases (Fig. 6A,B) are based on the detailed seismic profiling and gravity modeling of the Buckskin–Rawhide MCC and the surrounding Basin and Range [9,39]. The third reference case (Fig. 6C) uses our seismic constraints for relatively unextended crust (ABBY) and an average density for the crust in the region [Clem Chase, personal communication]. All three solutions for the MCC require a density decrease of 3% (2720–2784 kg/m^3) relative to the standard Basin and Range crust (2810 kg/m^3), the Buckskin–Rawhide MCC (2850 kg/m^3), and the relatively unextended case (2830 kg/m^3).

We consider differences in density distribution to be a major factor for the high elevation of the Catalina–Rincon and other MCCs in our study area. Relatively light crust beneath these features satisfies the observed gravity low while presenting a stable environment to maintain high elevation. Lower density crust atop normal density mantle would also produce the large seismic impedance contrast observed at the Moho on receiver functions. The alternative, a 1% less dense mantle of 3206–3233 kg/m^3 (noted in yellow, Fig. 6), would presumably generate a higher magnitude and longer wavelength gravity low that is unobserved and diminish the significant impedance contrast at the Moho. However a recent study by Abers et al. [40] indicates that lighter density mantle may provide a significant source of support for young MCCs and this finding prevents us from ruling out a mantle contribution in this case.

4.2. Compositional models

Comparing modeled densities to the compositions of MCC rocks helps to validate our model findings as well as include the independently constrained Vp/Vs estimates as we seek to determine the composition and

Fig. 6. Three isostatic model pairs for density structure. Crust and mantle are denoted with different shades. The left column of each pair is the reference case: (A) Buckskin–Rawhide MCC, (B) Basin and Range in southeastern Arizona, and (C) Station ABBY. The crustal value in the crust is the calculated density at the Catalina–Rincon MCC. The mantle value indicates the necessary density to produce the same observed gravity if the crust is kept as the reference density in each case.

Table 3
Average compositions and calculated seismic properties for the Oracle–Ruin granite (Yo), Leatherwood suite and equivalent (Kg*), Wilderness suite (Tw), and Catalina granite and equivalent (Tg*) intrusions in the Catalina–Rincon metamorphic core complex

Mineral Weight %	Yo	Kg*	Tw	Tg*
Quartz	33.0	17.8	28.4	34.5
K-Feldspar	28.0	7.3	29.2	35.3
Anorthite	14.0	17.5	6.5	6.4
Albite	14.0	27.9	28.1	16.6
Biotite	9.0	18.6	3.3	4.4
Muscovite	0.0	0.0	2.4	0.6
Hornblende	0.0	5.2	0.0	0.2
Other	0.0	4.9	0.9	1.2
ρ (kg/m3)	2664	2738	2650	2644
Vp (km/s)	6.04	6.12	6.06	6.03
Vs (km/s)	3.51	3.45	3.50	3.52
Vp/Vs	1.72	1.77	1.73	1.71

Compositions from Keith et al. [38].

means of support of the MCCs studied here. We apply the method of Hacker and Abers [41] to estimate rock composition near the area sampled by seismic measurements. Mapping and petrologic analysis of the Catalina–Rincon MCC show that the area is underlain by four distinct suites of intrusive bodies (Table 3); the region-wide Oracle granite (~1.4 Ga), the more locally exposed Leatherwood suite plutons (~75–65 Ma), Wilderness granite (~50–44 Ma), and Catalina granite and equivalents (~30–25 Ma) (see Keith et al. [42] for a summary). We compute average composition for each intrusion and model their seismic properties for mid-crustal conditions of 0.6 GPa and 400 °C. The results agree with the general results of Christensen [20]; that plagioclase content, along with variability of quartz and mafic minerals, significantly affects the seismic properties of a rock. The Leatherwood suite intrusions, corresponding temporally to significant late Cretaceous volcanic deposits exposed in the nearby Tucson Mountains [43], have a 3–4% increase in density and Vp/Vs ratio relative to the basement granitoids and succeeding intrusive episodes. The modeled Vp/Vs along with the seismically determined observations of abnormally high Vp/Vs at all MCCs surveyed here suggest that rocks with similar properties to the Leatherwood suite intrusions may constitute a substantial volume of the crust beneath the Catalina–Rincon MCC and possibly other MCCs in southern Arizona.

Although the modeled Vp/Vs ratio for the Leatherwood suite (1.77) exceeds that of the Oracle granite basement (1.72), Wilderness granite (1.73) and Catalina granite (1.71) it still fails to reproduce the value observed from receiver functions. As the higher Vp/Vs value within the Catalina–Rincon crustal block results from the prevalence of the anorthite and biotite-rich Leatherwood suite material, presumably similar, and possibly more plagioclase and mafic mineral-rich material exists at deeper levels. To test this hypothesis we create three models for deep crustal composition (Table 4), designed to explore the effects of adjusting specific mineral content at the same mid-crustal P–T conditions (0.6 GPa, 400 °C). Building upon the initial Leatherwood suite composition we test a material with 20% quartz, 5% K-feldspar, 30% anorthite, 20% albite, 20% biotite and 5% hornblende and using the Hacker and Abers [41] calculation arrive at a Vp/Vs ratio of 1.77 and a density of 2726 kg/m^3 which is still lower than our observed values for TUC/LEMN, KITT and SQRL. To determine a composition with a larger Vp/Vs value we eliminate K-feldspar and hold hornblende and biotite constant while decreasing quartz and increasing plagioclase. This material, approximate in composition to a quartz diorite, maintains a relatively low density (2741 kg/m^3) but has an increased Vp/Vs value (1.84). This final model has a density increase of 0.5% while the Vp/Vs has increased by 4%, illustrating that compositional changes can often influence Vp/Vs more noticeably than density. These results support the findings of Christensen [20] and illustrate the important connection between composition that varies by relatively minor amounts and large changes in the material Vp/Vs. The calculated Vp/Vs and density also match closely the seismically constrained Vp/Vs and isostatically modeled density (Figs. 3 and 6).

The constraints from our seismic observations and isostatic modeling allow us to estimate the lower crustal composition of the Catalina–Rincon MCC and, by similarity of seismic observations, the possible crustal composition for other MCCs in this study. There are several important points regarding these model results and

Table 4
Model compositions and calculated seismic properties for deep intrusions beneath the Catalina–Rincon metamorphic core complex

Mineral weight %	Model 1	Model 2	Model 3
Quartz	20	10	5
K-Feldspar	5	0	0
Anorthite	20	30	35
Albite	30	35	35
Biotite	20	20	20
Hornblende	5	5	5
ρ (kg/m^3)	2726	2737	2741
Vp (km/s)	6.05	6.15	6.21
Vs (km/s)	3.41	3.39	3.37
Vp/Vs	1.77	1.82	1.84

The Vp/Vs ratio changes show the significant effect of compositional variations on the seismic response of a material.

their implications. The estimated Vp of the crust for any actual or modeled composition does not exceed 6.21 km/s. This value is near the assumed 6.2 km/s wavespeed used for depth conversion of the receiver functions, and provides confidence in the crustal thickness and Vp/Vs estimates. Secondly, to produce the observed Vp/Vs values of the bulk crust at TUC/LEMN and SQRL, the intrusive bodies in the mid- to lower crust require a Vp/Vs ratio above ~1.90, higher than our models produce. It is also unknown how deformation and metamorphism have contributed to the composition of the lower crust. Finally, these results appear to form a paradox. The crustal column of Catalina–Rincon MCC has a high Vp/Vs ratio yet also is light enough to maintain its high elevation. The density—Vp/Vs trend calls for either a neutral or positive correlation for the compositions examined (Tables 3 and 4). Thus, density of the region surrounding MCCs may be as low or lower to coincide with lower observed Vp/Vs, though Moho Ps amplitude on receiver functions does not explicitly support this possibility. Because of this inferred density heterogeneity, the broken plate flexural model by Holt et al. [37] is especially appealing to explain this observation due to the fact that it decouples the uplifted Catalina–Rincon crustal block from the surrounding Basin and Range. A component of buoyancy in the mantle beneath MCCs in this region may also provide a source of buoyancy that cannot be explained by crustal density differences.

Another geodynamic model by Block and Royden [44] questions the applicability of Airy isostasy in MCC formation. Their model proposes that flowing lower crust in detachment systems moves laterally and vertically to fill voids created during extension, thus maintaining a flat Moho geometry while emplacing domes of lower crust material. Our seismic observations of a subhorizontal Moho support this hypothesis and flowing lower crust may provide a mechanism to create the Vp/Vs anomalies by transporting higher Vp/Vs material underneath a MCC from the surrounding regions. However, this process would presumably raise the density as well. Thus the applicability of this model relies on a balance between emplacing a sufficient amount of lower crust with a composition that would raise Vp/Vs, but not increase the density beyond our range of estimates. In this situation, crustal flow would have likely occurred long after emplacement of the high Vp/Vs Laramide age plutons. The tectonic practicality of such a model is beyond the scope of this study.

5. Concluding remarks

These new receiver function observations from the Colorado Plateau and Basin and Range illustrate the fundamental differences in crustal thickness, structure and composition between these tectonic provinces. Despite their geographic proximity it is clear from seismic observations that late Mesozoic and Cenozoic tectonic activity has imparted a pronounced difference in the seismic character of these regions. The upper lithosphere of the Colorado Plateau possesses greater crustal thickness, increased crustal layering, higher than average Vp/Vs values, areas of gradational Moho, and possible evidence of partial melt at both deep and shallow levels (Fig. 4, Table 2). The Basin and Range has thinner crust, lacks significant layering and contains observed Vp/Vs values that suggest an average crustal composition (Fig. 2, Table 1), except at MCCs where the Vp/Vs ratio is much higher than surrounding areas. Through extension the southern Basin and Range has maintained a crust of uniform thickness despite major differences in elevation and inferred through the Vp/Vs values, composition. The large variance in the Vp/Vs ratio differs from previous observations that suggest similar crustal compositions within the Basin and Range and Colorado Plateau (e.g., [13]).

Both seismic and gravity measurements of the MCCs imply the absence of a supporting root. Seismic observations also detect a sharp Moho and significantly higher Vp/Vs ratio than the surrounding Basin and Range. Modeling of crustal density for the Catalina–Rincon MCC results in a lower density crust than reference models based on the seismically constrained thicknesses. Our findings show that MCCs in the southern Basin and Range retain a substantial portion of their elevation due to a locally buoyant column of crust and possibly upper mantle. Results of compositional modeling (Table 4) allow us to speculate that the crust of the Catalina–Rincon MCC and its neighboring MCCs consists primarily of a plagioclase end-member anorthite-rich and quartz-poor material that may relate to the emplacement of the Leatherwood suite plutons during a significant Laramide-age magmatic episode. It also appears that magmatic or deformational processes during MCC formation may have sharply demarcated the crust—upper mantle transition as seen from high amplitude Moho Ps converted phases on receiver functions (Fig. 2).

It is important to consider that the anomalous Basin and Range Vp/Vs values are only related to areas that have undergone significant deformation and exhumation during the mid-Tertiary extension. We assert that Vp/Vs anomalies like those observed beneath the Catalina–Rincon MCC and others signify substantial variability in composition of the crust, and that these differences may have altered the distribution of strength in the crust and as a result primed certain areas for extension and exhumation during the process of orogenic collapse.

Acknowledgements

A special thanks goes to the COARSE team at both Arizona State and University of Arizona for their dedicated work during the installations, service runs, and database maintenance. We are grateful to numerous property owners, the Bureau of Land Management, National Forest Service, and National Park Service for granting us permission to use their land. We especially acknowledge the help of Gayle Zizzo of the Department of Geosciences, Bob Peterson of the University of Arizona Steward Observatory, John Dunlap and Claude Plymate at the Kitt Peak Observatory, John Ratje and John Waack at the Mt. Graham binocular telescope, and Bob and Kathy Minitti. We thank Drs. Mihai Ducea, Clem Chase, Roy Johnson, Jon Patchett, Randy Richardson, Trey Wagner, and Tom Owens for illuminating discussions concerning this study. We used software written by Chuck Ammon, Arda Ozacar and Clem Chase for the data analysis. Global Seismographic Network (GSN) is a cooperative scientific facility operated jointly by the Incorporated Research Institutions for Seismology (IRIS), the United States Geological Survey (USGS), and the National Science Foundation (NSF). The facilities of the IRIS Data Management System, and specifically the IRIS Data Management Center, were used for access to waveform and metadata required in this study. The IRIS DMS is funded through the National Science Foundation and specifically the GEO Directorate through the Instrumentation and Facilities Program of the National Science Foundation under Cooperative Agreement EAR-0004370. This work was made possible by funding from the National Science Foundation through the Graduate Research Fellowship Program, the IRIS Undergraduate Internship Program, and the University of South Carolina.

References

[1] W.R. Dickinson, Cenozoic plate tectonic setting of the Cordilleran region in the United States, in: J.M. Armentrout, M.R. Cole, H. TerBest (Eds.), Cenozoic Paleogeography of the Western United States, Pacific Section, . Soc. Econ. Pal. Min., 1979, pp. 1–13.

[2] P.J. Coney, T.A. Harms, Cordilleran metamorphic core complexes: Cenozoic extensional relics of Mesozoic compression, Geology 12 (1984) 550–554.

[3] L.J. Sonder, C.H. Jones, Western United States extension: how the west was widened, Annu. Rev. Earth Planet. Sci. (1999) 27417–27462.

[4] G. Zandt, S.C. Myers, T.C. Wallace, Crust and mantle structure across the Basin and Range—Colorado Plateau boundary at 37°N latitude and implications for Cenozoic extensional mechanism, J. Geophys. Res. 100 (1995) 10529–10548.

[5] J. Ligorria, C.J. Ammon, Iterative deconvolution of teleseismic seismograms and receiver function estimation, Bull. Seismol. Soc. Am. 89 (1999) 1395–1400.

[6] C.A. Langston, Structure under Mount Rainier, Washington, inferred from teleseismic body waves, J. Geophys. Res. 84 (1979) 4749–4762.

[7] T.J. Owens, S.R. Taylor, G. Zandt, Isolation and enhancement of the response of local seismic structure from teleseismic P-waveforms, Lawrence Livermore Laboratory Internal Report, 1983 33 pp.

[8] N.I. Christensen, W.D. Mooney, Seismic velocity structure and composition of the continental crust: a global view, J. Geophys. Res. 100 (1995) 9761–9788.

[9] J. McCarthy, S.P. Larkin, G. Fuis, R.W. Simpson, K.A. Howard, Anatomy of a metamorphic core complex: seismic refraction/wide-angle reflection profiling in southeastern California and western Arizona, J. Geophys. Res. 96 (1991) 12259–12291.

[10] D.H. Warren, A seismic refraction survey of crustal structure in central Arizona, Geol. Soc. Amer. Bull. 80 (1969) 257–282.

[11] Y.A. Sinno, G.R. Keller, M.L. Sbar, A crustal seismic refraction study in west-central Arizona, J. Geophys. Res. 86 (1981) 5023–5038.

[12] D.M. Gish, G.R. Keller, M.L. Sbar, A refraction study of deep crustal structure of the Basin and Range—Colorado Plateau transition zone in eastern Arizona, J. Geophys. Res. 86 (1981) 6029–6038.

[13] T. Parsons, J. McCarthy, W.M. Kohler, C.J. Ammon, H.M. Benz, J.A. Hole, Crustal structure of the Colorado Plateau, Arizona: application of new long-offset seismic data analysis techniques, J. Geophys. Res. 101 (1996) 11173–11194.

[14] L. Zhu, H. Kanamori, Moho depth variation in southern California from teleseismic receiver functions, J. Geophys. Res. 105 (2000) 2969–2980.

[15] H. Gurrola, J.B. Minster, T.J. Owens, The use of velocity spectrum for stacking receiver functions and imaging upper mantle discontinuities, Geophys. J. Int. 117 (1994) 427–440.

[16] S.C. Myers, S.L. Beck, Evidence for a local crustal root beneath the Santa Catalina metamorphic core complex, Arizona, Geology 22 (1994) 223–226.

[17] G. Zandt, C.J. Ammon, Continental crust composition constrained by measurements of crustal Poisson's ratio, Nature 374 (1995) 152–154.

[18] D.J. Lynch, Neogene Volcanism in Arizona—The recognizable volcanoes, in: J.P. Reynolds, J.P. Jenney (Eds.), Geol. Soc. Digest, vol. 17, Geologic evolution of Arizona, Tucson, Arizona, 1989, pp. 681–700.

[19] G.S. Lister, S.L. Baldwin, Plutonism and the origin of metamorphic core complexes, Geology 21 (1993) 607–610.

[20] N.I. Christensen, Poisson's ratio and crustal seismology, J. Geophys. Res. 101 (1996) 3139–3156.

[21] E.C. Hauser, J. Lundy, COCORP Deep reflections: Moho at 50 km (16 s) beneath the Colorado Plateau, J. Geophys. Res. 94 (1989) 7071–7081.

[22] J. Chmielowski, G. Zandt, C. Haberland, The Central Andean Altiplano–Puna magma body, Geophys. Res. Lett. 26 (1999) 783–786.

[23] K.E. Sheetz, J.W. Schlue, Inferences for the Socorro magma body from teleseismic receiver functions, Geophys. Res. Lett. 19 (1992) 1867–1870.

[24] H. Gilbert, A. Velasco, G. Zandt, Preservation of Proterozoic terranes within the Colorado Plateau: a source of strength? First

Annual Earthscope National Meeting, Santa Ana Pueblo, NM, 2005.
[25] K.L Tanaka, E.M Shoemaker, G.E. Ulrich, E.W. Wolfe, Migration of volcanism in the San Francisco volcanic field, Arizona, Geol. Soc. Amer. Bull. 97 (1986) 129–144.
[26] T.C. Moyer, L.D. Nealey, Compositional regional of variations late Tertiary bimodal rhyolite lavas across the Basin and Range/Colorado Plateau boundary in western Arizona, J. Geophys. Res. 94 (1989) 7799–7816.
[27] N. Beghoul, M. Barazangi, Mapping high Pn velocity beneath the Colorado Plateau constrains uplift models, J. Geophys. Res. 94 (1989) 7083–7104.
[28] C.G. Chase, J.C. Libarkin, A. Sussman, Colorado Plateau: geoid and means of isostatic support, Int. Geol. Rev. 44 (2002) 575–587.
[29] P. Morgan, C.A. Swanberg, On the Cenozoic uplift and tectonic stability of the Colorado Plateau, J. Geodyn. 3 (1985) 39–63.
[30] M. Roy, J.K. McCarthy, J. Selverstone, Upper mantle structure beneath the eastern Colorado Plateau and Rio Grande rift revealed by Bouguer gravity, seismic velocities, and xenolith data, Geochem. Geophys. Geosyst. 6 (2005), doi:10.1029/2005GC001008.
[31] J. Spencer, Uplift of the Colorado Plateau due to lithosphere attenuation during Laramide low-angle subduction, J. Geophys. Res. 101 (1996) 13595–13609.
[32] M. West, J. Ni, W.S. Baldridge, D. Wilson, R. Aster, W. Gao, S. Grand, Crust and upper mantle shear wave structure of the southwest United States: implications for rifting and support of high elevation, J. Geophys. Res. 109 (2004), doi:10.1029/2003JB002575.
[33] J.D. Hendricks, J.B. Plescia, A review of the regional geophysics of the Arizona transition zone, J. Geophys. Res. 96 (1991) 12351–12373.
[34] L.A. Lastowka, A.F. Sheehan, J.M. Schneider, Seismic evidence for partial delamination model for Colorado Plateau uplift, Geophys. Res. Lett. 28 (2001) 1319–1322.
[35] H.J. Gilbert, A.F. Sheehan, Images of crustal variations in the intermountain west, J. Geophys. Res. 109 (2004), doi:10.1029/2003JB002730.
[36] R.W. Simpson, R.C. Jachens, R.J. Blakely, R.W. Saltus, A new isostatic residual gravity map of the conterminous United States with a discussion on the significance of isostatic residual anomalies, J. Geophys. Res. 91 (1986) 8348–8372.
[37] W.E. Holt, C. Chase, T. Wallace, Crustal structure from three-dimensional gravity modeling of a metamorphic core complex: a model of uplift, Santa Catalina–Rincon mountains, Arizona, Geology 14 (1986) 927–930.
[38] R. E. Sweeney, P. L. Hill, Arizona Aeromagnetic and Gravity Maps and Data: A Web Site for Distribution of Data, U.S.G.S. Open File Report 01-0081 (2001).
[39] T. Parsons, J. McCarthy, G.A. Thompson, Very Different Crustal Response to Extreme Extension in the Southern Basin and Range and Colorado Plateau Transition, in: M.C. Erskine, J.E. Faulds, J. M. Bartley, P.D. Rowley (Eds.), Am. Assoc. Pet. Geols., Pacific Section, Guidebook, vol. 78, 2001, pp. 291–304.
[40] G.A. Abers, A. Ferris, M. Craig, H. Davies, A.L. Lerner-Lam, J.C. Mutter, B. Taylor, Mantle compensation of active metamorphic core complexes at Woodlark rift in Papua New Guinea, Nature 418 (2002) 862–865.
[41] B.R. Hacker, G.A. Abers, Subduction Factory 3: an excel worksheet and macro for calculating the densities, seismic wave speeds, and H_2O contents of minerals and rocks at pressure and temperature, Geochem. Geophys. Geosyst. 5 (2004), doi:10.1029/2003GC000614.
[42] S.B. Keith, S.J Reynolds, P.E. Damon, M. Shafiqullah, D.E. Livingston, P.D. Pushkar, Evidence for multiple intrusion and deformation within the Santa Catalina–Rincon–Tortolita crystalline complex, southeastern Arizona, in: M.D. Crittenden, P.J. Coney, G.H. Davis (Eds.), Cordilleran Metamorphic Core Complexes, Geol. Soc. Am. Memoir., vol. 153, 1980, pp. 217–267.
[43] W.R. Dickinson, Tectonic setting of faulted Tertiary strata associated with the Catalina core complex in southern Arizona: special paper, Geol. Soc. Amer. Bull. 264 (1991) 106.
[44] L. Block, L.H. Royden, Core complex geometries and regional scale flow in the lower crust, Tectonics 9 (1990) 557–567.